

Nanostructural model of metal-insulator transition in layered Li_xZrNCl superconductors

J. C. Phillips

Department of Physics and Astronomy, Rutgers University, Piscataway, New Jersey 08854-8019, USA

(Received 7 June 2007; published 31 March 2008)

The self-organized dopant percolative filamentary model, entirely orbital in character (no fictive spins), has recently quantitatively and specifically explained chemical trends in ceramic layered cuprate superconductors. Here, this model explains the observation of an abrupt jump $\Delta T_c(x)$ in Li_xZrNCl powders over a wide composition range Δx , as well as many other features in the resistivity, lattice constants, Raman spectra, upper critical field, and Meissner volume factor. The ceramic data confirm one-dimensional features in realistic structural models of three-dimensional metal-insulator transitions that had been previously only hypothetical. These data provide a “missing link” between the metal-insulator transition in semiconductor impurity bands and cuprate superconductors. They show that all three material families are united by exhibiting an intermediate phase, absent from crystals, but seen in many properties of network glasses.

DOI: [10.1103/PhysRevB.77.104534](https://doi.org/10.1103/PhysRevB.77.104534)

PACS number(s): 74.70.-b

I. INTRODUCTION

The discovery of high-temperature superconductivity (HTSC) in ceramic cuprates¹ has stimulated investigators to search for superconductivity in other ceramic compounds. Whereas layered cuprate superconductivity usually relies on oxygen doping, other layered ceramic nitrochlorides doped by lithium also become superconductive, although at lower T_c . In particular, the titled materials show² T_c around 15 K, or when Zr is replaced by Hf, 25 K,³ over a wide range of x .

Layered Li_xZrNCl exhibits [Fig. 3(b) of Ref. 4] a metal-insulator transition (MIT) near $x=x_c=0.06$ which closely resembles the archetypical MIT seen in three-dimensional semiconductor impurity bands (Si or Ge, doped by B, P, or As). An abrupt decrease ΔT_c in T_c from 15 to 12 K also occurs in Li_xZrNCl [Fig. 4(b) of Ref. 4] in the Δx composition range between x_c and $2x_c$. Over this same range, the low-temperature normal state conductivity σ (in a magnetic field that suppresses superconductivity) is proportional to $(x-x_c)^\alpha$, with $\alpha=0.5$, the same value as was observed in semiconductor impurity bands.

Many attempts were made to explain $\alpha=0.50$ in semiconductor impurity bands by using continuum models, treating the conductivity in terms of critical fluctuations.⁵ Such fluctuation models are valid only for the *narrow* range of $\delta x/x_c=(x-x_c)/x_c \leq 10^{-2}$, so continuum critical fluctuation models simply cannot explain the *observed* wide range of $\Delta x/x_c \sim 1$. (For the case of truly randomly distributed impurities in neutron-transmutation doped semiconductor impurity bands, the range of concentrations where critical fluctuations occur is only 0.0015, and in that very small range, $\alpha = 1/3$, not $1/2$.⁵ Thus using critical fluctuation models to describe the observed wide range of $\Delta x/x_c \sim 1$ is simply wrong. Materials science may be less rigorous than pure mathematics, but it is not 100 times less rigorous!) The data on ΔT_c and $\sigma(x-x_c)$ were discussed in Ref. 4 by using these mathematically questionable and physically confusing continuum models (which contain only one phase transition), with the result that many aspects of the data, such as the abrupt rise in T_c beginning at 12 K, were left unexplained. Instead, a quantum (not classical) percolation model,⁶⁻⁸

which provided a natural explanation of the semiconductor impurity band data, is much more appropriate. Percolation is *qualitatively different* from critical fluctuations, as it involves one-dimensional filaments embedded in a three-dimensional medium. As we shall see, the percolation model explains all the features of the data that the continuum “critical fluctuation” model failed to explain.

Most importantly, not only for the metal-insulator transition in semiconductor impurity bands but also in many other glassy networks,⁸ a filamentary *intermediate phase* was identified,⁸ which is completely different from a critical point. The intermediate phase is associated with nonequilibrium situations, and it reflects the fact that the impurity configuration is strongly disordered (a frozen-in glass). This glassy model also works well here for the observed wide range of $\Delta x/x_c \sim 1$, and it leads to the identification of two (not just one) phase transitions. This structural model clarifies the content of the Li_xZrNCl data. It shows that the latter ceramics occupy an important global position, as a “missing link” located between the intermediate phase in semiconductor impurity bands and the intermediate phase responsible for cuprate HTSC.

II. CONTINUUM MODELS

Layered and hexagonal TiO_2 is much studied for applications as an electrode for solar cells because of its high capacity for, and ease of, Li intercalation. Electronic structure calculations⁹ have shown that upon Li insertion, the host lattice undergoes large deformations, which can be related to the excitation of soft vibrational modes. Donation of Li charge to the host TiO_2 lattice increases the radii of acceptor Ti ions and causes anisotropic volume expansion. By using a model that allows charge transfer among ions, molecular dynamics simulations¹⁰ showed that lithium diffusion occurs through jumps between octahedral sites located along channels parallel to the [001] direction.

The ZrNCl structure consists of double honeycomb hexagonal ZrN bilayers sandwiched between Cl layers, and Li is intercalated (assisted by organic molecular carriers, which pry the sandwiches apart) between the weakly bound sand-

wiches and Cl layers. One can regard this material as chemically derived from TiO_2 by replacing Ti^{4+} by Zr^{4+} and splitting the O_2^{2-} planes into valence-charge conserving N^{3-} and Cl^- planes. To overcome the strong ionic Li-Cl interactions in powders, Li is intercalated with an organic molecule (for example, tetrahydrofuran, $\text{C}_4\text{H}_8\text{O}$, a moderately polar, aprotic solvent). Even at the low doping level of $x=0.16$, Li intercalation both donates carriers to the ZrNCl sandwiches and produces a different stacking sequence of the Zr-N double layers along the c axis, also visualized by a shift of Zr-N double layers within the x - y plane relative to each other.¹¹ This surprising shift is explained by an increase in the radii of Zr ions after acceptance of charge donated by Li intercalation. In this double honeycomb hexagonal structure, each Zr ion is surrounded by three coplanar honeycomb N ions and one short-bonded N ion (labeled N_{cap}) in the adjacent shifted honeycomb layer. Thus, it is not surprising that single crystals have been synthesized only for $x=0$ and under high pressure.¹² The undoped ZrNCl single crystal structure is described in terms of filling of ZrCl with N layers, with Zr-N bond lengths much shorter than in ZrN (NaCl structure).

The pseudopotential band structure of the parent compound was calculated¹¹ assuming that these ZrNCl sandwiches are ideal. The band structure shows a conduction band minimum with a small effective mass $m^*/m=0.66$ and a correspondingly small $N(E_F)=0.33/\text{eV}$ spin cell. With this small density of states and a calculated value of the electron-phonon coupling constant $\lambda=0.5$, as well as a “normal metallic” value for the Coulomb repulsion parameter $\mu=0.1$, the calculated value of T_c is found to be only 5 K, or too small by a factor of 3. This is unsatisfactory in its own right, but even worse is the failure of the ideal model to predict the rapid rise of $T_c(x)$ between $2x_c$ and x_c of $\Delta T_c=3$ K [the band model predicts little or no composition dependence of $T_c(x)$ between $x=x_c$ and $x=1/3$].

Worse still, the isotope effect for N atoms is only 0.07, and to fit this requires $\mu>0.12$, which would give $T_c \sim 3$ K (Fig. 9 of Ref. 11). The overall lattice vibration spectrum appears to agree well with the spectrum determined by neutron scattering, apart from small opposite shifts of the acoustic (ZrN) and optic (Cl) modes, attributed to overestimation by 10% of dynamical couplings between the light N atoms and the heavy Zr and Cl atoms. However, there is still another problem: the (x, y) Cl optic modes should be narrow, as calculated, because there is little \mathbf{k} dependence in the coupling between the Cl plane and the doubled Zr,N planes, but experimentally, the upper two (x, y) Cl bands are about three times wider than the calculated bands, while all the other band widths (especially the acoustic band widths, where force cancellations are largest, and the greatest modeling errors usually occur) are in good agreement (Fig. 4 of Ref. 11). This suggests that there is substantial disorder somewhere in the (x, y) planes, especially the Cl planes, even in the undoped samples.

There are still more serious problems with ideally ordered continuum models. The lattice parameters of $M_x\text{ZrNCl}$ change by only $\sim 1\%$ when $M=\text{Zr}$ is replaced by $M=\text{Hf}$.³ Such small changes will change the band structure also by $\sim 1\%$, and at the end of the calculation, T_c itself will have

changed by $\sim 1\%$, not by nearly a factor of 2, as experimentally observed. *Most important of all*, while LiTiO_2 in the cubic spinel structure is also superconductive with $T_c=11.4$ K, the electronic specific heat coefficient γ of $\text{Li}_{0.12}\text{ZrNCl}$ is $<5\%$ of γ of LiTiO_2 ,¹³ which implies an averaged bulk $N(E_F)$ that is a factor of >2 too small to explain the observed T_c , or a value of the electron-phonon coupling constant $\lambda<0.22$. The inferred value of $2\Delta_0$ is ~ 60 K, which reasonably agrees well with a tunneling measurement,¹⁴ but the superconductive suppression of the specific heat γ disappears in a magnetic field of only 1 T, whereas magnetization measurements show $H_{c2}=5$ T. These many discrepancies between theory and experiment are not merely technical accidents; instead, they indicate a fundamental failure of the theory in modeling the experimental situation.

III. NANOSTRUCTURAL MODEL

At this point, there are two choices: one can appeal to some kind of exotic Coulomb interaction involving mysterious bosons^{11,13} (although it is hard to see how such an interaction would resolve the contradictions discussed above, especially the factor γ being two times too small, and the doubling of T_c when $M=\text{Zr}$ is replaced by $M=\text{Hf}$) or one can simply abandon the continuum model. The latter *assumes* that ZrNCl can be represented by an idealized lattice structure, which ignores the Li ions altogether, and which treats their additional carriers by a rigid band model. These sweeping assumptions are unavoidable if one wants to use band-theory methods to calculate electronic structure properties and the BCS theory to evaluate parameters such as γ . In general, these methods have been very successful for simple materials with stable structures, such as MgB_2 .¹⁵ However, the anomalously small γ is a strong signal that superconductivity and the MIT in Li_xZrNCl may well be better described by the *nanoscopically inhomogeneous* filamentary quantum percolation model^{16,17} that has proved to be so successful for cuprate HTSC and for deriving $\alpha=0.5$ over the wide range of $\Delta x/x_c \sim 1$ for semiconductor impurity bands.⁶ In this model, there are two phase transitions, rather than one, and between them there is an *intermediate topological phase* based on a filamentary network, not merely one phase transition with critical fluctuations.⁵ The strains associated with this intermediate phase, which are often observed with current high resolution Raman spectroscopy, characteristically exhibit two (not only one) phase transitions.¹⁷

Formally, one can treat the Zr-N bilayer shift instability by using the Zr- N_{cap} z coordinate (which reverses sign when x goes from 0 to 0.16) as an (x, y) planar variable that correlates with the (x, y) coordinates of the nearest Li dopants: this correlation will determine filamentary paths. The paths will determine filaments of maximum conductivity through minimum scattering. The latter will be minimized by minimizing Zr- N_{cap} z coordinate fluctuations, that is, by minimizing gradients of local Zr- N_{cap} z coordinates tangential to, and coplanar with, filaments.

An approach of this kind has already worked very well on Ag fast ion glassy solid electrolytes,¹⁸ which in the area of

ionic transport are just as spectacular as HTSC are for electronic transport. There, the topological (or hydrodynamic¹⁷) approach based on identifying the Lagrangian filaments is very successful. The filaments are composed of structural units with free volumes \mathfrak{F} above average, and are smoothly self-organized to minimize free volume differences $\delta\mathfrak{F}$ between successive filamentary cells, which minimizes scattering due to density fluctuations. Large-scale numerical simulations then predict ionic conductivities over 11 orders of magnitude and show that the activation energy E_σ for ionic conduction (analogous to a pseudogap or superconductive gap energy) scales with $\mathfrak{F}^{d/3}$, with $d=1$. For Li_xZrNCl , one replaces $\delta\mathfrak{F}$ by δz , and the main features of the topology will not change.

For layered compounds, the most obvious nanoscopically inhomogeneous planar channel model is the one that contains “hard” semiconductive nanodomains embedded in a soft matrix of filamentary nanodomain walls, made metallic by doping by proximate Li ions. Such a matrix, with buckling in the Cl planes at nanodomain interfaces, effectively relieves interlayer stresses in much the same way as misfit dislocations relieve epitaxial misfit stresses at semiconductor interfaces. For the cuprates, this analogy was quite fruitful, as it led to the prediction^{16,19} of nanodomains with 2–4 nm diameters *before* these were discovered by scanning tunneling microscopy (STM)²⁰ on single crystals of the micaceous layered soft cuprate $\text{Bi}_2\text{Sr}_2\text{CaCu}_2\text{O}_{8+x}$ (BSCCO). It unlikely seems that similar STM studies can be made on superconductive layered soft Li_xZrNCl (so far prepared only as powders), so we are fully justified in assuming that similar nanodomain structures are formed, indexed by the $\text{Zr-N}_{\text{cap}} z_{\text{cap}}$ coordinate. This “broken translational symmetry” model is further supported by the wide range (2.14–2.49 Å) of values of the $\text{Zr-N}_{\text{cap}} z$ coordinate measured by different authors.¹²

The first point to be noted about the nanodomain model is that an abrupt variation in z_{cap} at the boundary of a nanodomain will always reflect the Bloch waves and that there could be a Jahn–Teller gap opened at the boundary by atomic relaxation; we do not need to know the details of this relaxation to see that a pseudogap will form. To explain the anomalously small value of γ , this pseudogap needs only to reduce the local density of states at E_F associated with the nanodomain interiors. Moreover, Fermi-energy pinning metallic impurity band states can form within this gap associated with nearby Li dopants. Then, if the nanodomains fill $\sim 50\%$ of the sample volume, only 50% of the material in the walls between the nanodomains will be metallic, and the reduction in γ is readily explained. (Assuming that this equal separation is correct, one obtains a nanodomain diameter of about 2 nm.) Moreover, with the breakdown of translational invariance, the electron-phonon interactions with momentum transfer \mathbf{q} , which are restricted to small regions of \mathbf{q} space in idealized lattice models,¹¹ are freed, and the way is opened for the much stronger interactions needed to increase the electron-phonon coupling strength λ and increase $2\Delta_{0r}/kT_c$ from the BCS value of 3.5 to the observed value of 5.¹³ In fact, as the filamentary metallic material is both softened between the hard pseudogap nanodomains, and supported by them against further Jahn–Teller distortions, we would expect stronger electron-phonon coupling strengths λ to be

achievable in the metallic filamentary material.

One of the strongest attractions of the nanodomain misfit model is that it explains how small changes in MN layer parameters can nearly double $T_c(M)$ from $M=\text{Zr}$ to $M=\text{Hf}$. The misfit that occurs between the effective (sometimes called prototypical) lattice constants of the MN plane and the Cl plane can be (and for semiconductor heterointerfaces is always) of the order of a few percent or less. For Li_xMNCl , when M changes from Zr to Hf, it was not possible to determine the change in the M -N bond length or the M -N- M bond angle in powder samples.³ It likely seems that nanodomain misfit of M -N planes with the Cl planes (fixed prototypical lattice constant) is driven by M - M bonding, previously identified as being the critical factor for achieving $T_c > 10$ K in borides, nitrides, sulfides, and selenides.²¹ That misfit could even create defects in the Cl plane, for instance, buckling of the latter at M -N domain walls, leading to good localization of bare Li ions. Moreover, if the nanodomain misfit is driven by M - M bonding, it is also easy to understand why the N isotope effect on T_c is so small.¹¹

Broken translational symmetry and filamentary nanodomain interfaces also explain the rapid reappearance of the specific heat γ at only $H=1$ T.¹³ The Abrikosov vortices associated with $H_{c2}=5$ T appear on a large scale of ~ 100 nm, and they require only a small fraction of intact superconductive filaments, consistent with destruction of the superconductive gap in the rest of the filaments by the 1 T magnetic field. Because the filaments are quasi-one-dimensional, their phase coherence and superconductivity are fragile and easily destroyed by the Lorenz forces. This fragility is quite similar to the universal “upward positive (nonsaturating) curvature” of $H_{c2}(T)$ observed in single crystals or thin films of the layered cuprates, where the magnitude of the positive curvature and the magnetic-field quenching of the specific heat is largest in the materials with the most anisotropic resistivity.²² Such a correlation is compatible with the zigzag interlayer filamentary percolative model for the cuprates,^{16,33} which emphasizes the key role played by dopant-centered interlayer currents.

According to microscopic theory,²³ there are two possible causes for rapid magnetic-field quenching of superconductivity. Both are based on reducing the coherence length, which can be done either by spin scattering or by orbital reflection at nanodomain walls. (In hard continuum models without spins and/or nanodomains, the curvature of $H_{c2}(T)$ is always negative.) In the early days of cuprates, it turned out to be difficult to separate spin scattering from orbital vortex reflection at nanodomain walls because the parent insulators are often antiferromagnetic, and it is difficult to exclude the possibility that the pseudogap could be caused by spin waves. (However, recently, the tide in cuprates has been very strongly running in favor of pseudogaps being caused by Jahn–Teller distortions or charge density waves.¹⁷) In the case of the TiO_2 or Li_xMNCl family, there is no antiferromagnetism, but there is strong evidence for nanodomain formation, which provides a simple and unambiguous explanation of the observed “soft” or “fragile” field-quenching effects.

IV. NANONETWORK METAL-INSULATOR TRANSITION

The broad trend of $T_c(x)$ is very similar for all the alkali metals A intercalated into $A_x\text{MnCl}$: $T_c(x)$ is flat from $x=0.16$ up to $x\sim 0.5$, and then it slowly decreases to 10 K at $x\sim 1.4$. The knee at $x\sim 0.5$ suggests some ordering of the Li dopants, which is in registry with the hexagonal honeycomb MnCl substrate, possibly through 2×1 short-range order. For small x , the jump of $\Delta T_c=3\text{ K}\sim T_c/4$ between $2x_c$ and x_c occurs in the same concentration range where the conductivity is proportional to $(x-x_c)^\alpha$, with $\alpha=0.5$; this striking behavior, together with the jump of ΔT_c , was observed⁴ only after the *n*-butyl Li ($\text{CH}_3\text{CH}_2\text{CH}_2\text{CH}_2\text{Li}$) intercalated samples were annealed at 600°C for 30 min, which presumably removed the cointercalated organic molecular carrier [here, as hexane, $\text{CH}_3(\text{CH}_2)_4\text{CH}_3$]. The authors suggest that this annealing promoted a single-phase structure for low x . Another, and more specific, possibility is that the large organic molecular carrier $\text{CH}_3\text{CH}_2\text{CH}_2\text{CH}_2$ immobilized the Li dopants and prevented them from localizing very near the narrow nanodomain edges of the ZrNCl substrate, effectively suppressing filamentary network coherence between these edges by interactions with disordered Li-organic molecule complexes. Removal of interlayer organic molecules reduces the length scale for dopant ordering and allows the Li ions to assume quasiperiodic configurations that promote formation of coherent nanodomain wall “wires.”

In semiconductor impurity bands, the power-law fit to the conductivity at the MIT with $(x-x_c)^\alpha$, $\alpha=0.50$, is successful⁶ over a very wide range, $0.01 < \Delta x/x_c < 1$. (Note that classical percolation⁷ in two dimensions gives $\alpha=1.3$. So far, all three-dimensional simulations have used only lattice models and have never obtained $\alpha < 1$. Quantum percolation⁶ in three dimensions gives $\alpha=0.50$; the reason for this success is discussed further in Sec. V. It is well known⁶ that critical fluctuation theory is applicable only in the range $\delta x/x_c < 0.01$, so the analysis of the semiconductor impurity band MIT by using critical fluctuations⁵ is fundamentally unjustifiable and quite misleading. By contrast, the quantum percolation model not only gives $\alpha=0.50$, but it also successfully describes $d=3$ semiconductor impurity band conductivity over the wide range experimentally observed.⁶ The upper end of the range ($\sim 2x_c$) is related to a second phase transition from states localized near impurities to delocalized continuum states; this second transition is identifiable by a break in slope of the specific heat²⁴ as a function of x . The percolation viewpoint also successfully describes the effects of inhomogeneities in cuprate relaxation.²⁵

For the case of Li_xZrNCl , one can estimate the upper end of the percolative range as follows. One expects coherent percolation along paths of single filaments. Now, I assume that it is energetically favorable to have only $n=1$ (single) and $n=2$ (double) filaments for $x/x_c < 2$ because harmonic strain energy (the source of misfit reconstruction) increases such as n^2 ; the channel occupation is optimized just at $x=x_c$, where the number of single filaments is maximized, and coherence is lost by interfilamentary scattering as soon as each channel is fully occupied by two filaments. Then, coherent filamentary percolation will quite abruptly stop near $x=2x_c$, which appears to occur for $T_c(x)$ in Fig. 4(b) of Ref. 4.

Global network properties are indicated in the lattice constant functions $a(x)$ and $c(x)$ [Fig. 1(c) of Ref. 4 and the Raman spectra (Fig. 2 of Ref. 4 and Fig. 1 of Ref. 25)]. The Raman spectra²⁶ contain five ZrNCl phonon bands, labeled $A(x), \dots, E(x)$. The most striking feature of these five bands is that they are clearly divided into two subsets: I(B,E) and II(A,C,D). The frequencies of I(x) are almost independent of x , while the reduced frequencies of II(x) show parallel complex behavior soon to be discussed. First, can one explain the existence of two such well-defined subsets. This is an example of supersymmetry, which is possible because the Li is nearly randomly distributed on appropriate length scales. In other words, the Li dopants form a branched, filamentary network. The network is necessarily glassy, and all glasses are isotropic (except for scaling normal to planar directions). In that case, there are only two directions: longitudinal and transverse (parallel and normal to the local filamentary tangent). Because metallic filamentary currents are longitudinal, II(x) represents phonons longitudinally polarized, while I(x) phonons are polarized normal to the nanodomain walls. Naturally, the frequencies of I(x) are insensitive to variations in x .

In the parallel phonons, II(x) all show two features. First, between x_c and $2x_c$, their frequencies linearly soften (with $<0.3\%$ scatter) with x (just as in network glasses¹⁷) by 5% (a large amount, considering that the Li ions are only weakly coupled to the ZrNCl layers), with a large break in slope at $x=2x_c$. Second, the II(x) frequencies recover to reach a second peak between $x=0.13$ and 0.16 . This second peak probably represents a Zallen–Scher percolation threshold of larger-scale clusters associated with the *Z-S* magic fraction of 0.16 .²⁷ These two percolative features are also apparent (when one already knows from the Raman spectra where to look) in the lattice constants as upward tics in both $a(x)$ and $c(x)$ at $x=0.06=x_c$, a dip in $a(x)$ at $2x_c$, and strong dips in $a(x)$ and especially $c(x)$ at $x=0.16$. Also, Fig. 4b of Ref. 26 shows that the width of band E rapidly increases with x and has an inflection point near $x=2x_c$, as one would expect from enhanced electron-phonon scattering once the channels lose their one-dimensional character and scattering can occur over a wide range of planar angles. Overall, these structural data exhibit features of a soft network,^{6,17} which are entirely unexpected in hard continuum models.⁵

Finally, with the present fragile nanonetwork model in hand, one would expect that the Meissner volume fraction would reach a maximum at $x=2x_c$, and a local minimum at $x=0.16$, because the nanonetwork is full at $x=2x_c$, and the Zallen–Scher clusters disrupt the nanonetwork (although on a different length scale, so that their effects are small). All these aspects are indeed present in Fig. 4 (b) of Ref. 4. None of these effects can be explained by hard continuum models based on critical fluctuations.⁵

V. QUANTUM NATURE OF THE SCALING PHASE

Apart from the many features of Li_xMnCl that are puzzling from the point of view of hard continuum models (all explained, at least qualitatively, by the present soft or fragile nanoscopic model), there are two very surprising results: the

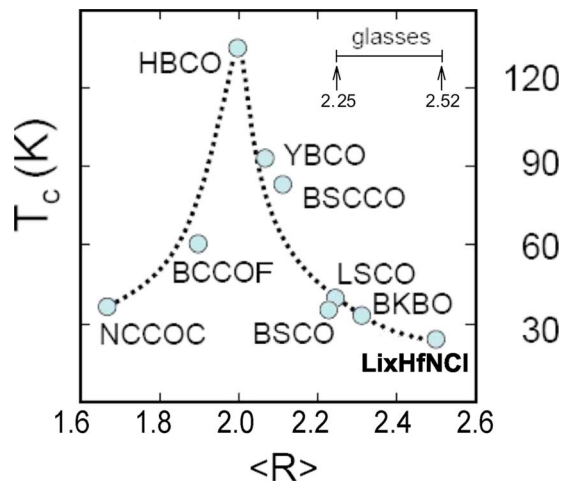


FIG. 1. (Color online) Chemical trends in T_c^{\max} with $\langle R \rangle = \langle |Z| \rangle$, which measures the global stiffness of the doped crystalline network, with $Z(\text{Cu})=2$, $Z(\text{Bi})=3$ (4) [BSCCO ($\text{Ba}_{1-x}\text{K}_x\text{BiO}_3$), as in the parent insulators, where $\Sigma Z=0$], and $Z(\text{O})=-2$. Perovskites ($R=2.40$) and pseudoperovskites are only marginally stable mechanically (Ref. 17), and for HTSC cuprates, $\langle R \rangle$ lies in the region of floppy networks just below the isostatic (rigid but unstressed) range determined by studies of network glasses (wavy line). The peak in T_c^{\max} occurs at $\langle R \rangle=2$, as one would expect from mean-field percolation theory. Note that the point for Li_xZrNCl , added here, lies on the extrapolation of the cuprate curve previously published in Ref. 17, showing that the superconductive properties of Li_xZrNCl are probably well described by the floppy network model successfully used for the cuprates (Ref. 17).

doubling of T_c from $M=\text{Zr}$ to $M=\text{Hf}$, with only $\sim 1\%$ structural change, and the appearance of the MIT with the conductivity proportional to $(x-x_c)^\alpha$, $\alpha=0.5$.

First, consider the near doubling of T_c from $M=\text{Zr}$ to $M=\text{Hf}$. This result is inexplicable in hard continuum models based on ideal lattices, but it becomes plausible in terms of the least upper bounds T_c^{\max} (the largest value of T_c for a given alloy family, at $P=0$) in the cuprates.¹⁷ As shown in Fig. 1, $\langle R \rangle$, the average number of the Pauling resonating bonds R in Li_xMNCl with $R(\text{M})=4$, $R(\text{N})=3$, and $R(\text{Cl})=1$, is just $8/3=2.65$ [if we include a small correction for $x=0.06$ with $R(\text{Li})=1$]. Then, $T_c^{\max}(\text{Li}_x\text{MNCl})=25$ K exactly lies on the cuprate curve extrapolated from $\langle R \rangle$ near 2. This means that both the cuprates and Li_xMNCl are marginally stable (soft) networks, which is consistent with the known softness of the TiO_2 rutile family,⁹ as well as the ability to intercalate large organic Li-carrying molecules between the Cl layers, in spite of the strong ionic interactions between Li and Cl. This softness also produces misfit nanodomains.

Next, consider the MIT with the conductivity proportional to $(x-x_c)^\alpha$, $\alpha=0.5$. Previously, this sublinear power law had been observed over the very wide range of $0.01 < \Delta x/x_c < 1$ only in three-dimensional semiconductor impurity bands,⁶ and there the conditions for its observation were very strict: the impurities must be randomly distributed, and this could be achieved only in a few cases, where the substitutional strain is small (Si or Ge, doped by B, P, or As). The nanodomain model of Li_xMNCl assumes the presence of misfit strains large enough to break down the MIT power law

in semiconductor impurity bands, which is an apparent inconsistency.

First, consider the details of the quantum percolation model⁶ for Li_xMNCl . Because we are interested in a wide range of $x > x_c$, we treat this range as an equilibrated, stress-free self-organized intermediate phase.¹⁷ In such phases, the number N of soft (cyclical) modes (here, identified with metallicly doped, softened nanodomain walls with no energy gap) is given as $N \sim x - x_c$ over a wide range of $x > x_c$.²⁸ The conductivity σ is proportional to Nl , where l is the mean free path, which, in turn, is inversely proportional to the scattering rate. The latter is proportional to the density of states $N(E_F)$, which near the band edge is proportional to $(x-x_c)^\beta$, with $\beta=(d-2)/2$. Then, $\sigma \sim Nl \sim (x-x_c)^{1-\beta}$, and $\alpha=2-d/2=0.5$ for $d=3$. This value of $d=3$ reflects the fact that the branched system (domain walls + Li) is three dimensional. In this calculation, the number N of metallic carriers (electrons that see no energy gap) is classically treated because it is identified with the number N of cyclical modes. The Fermi statistics enter the calculation of l through $N(E_F)$.

How can this hybrid classical-quantum model be extended to the case of randomly distributed impurities in three-dimensional semiconductors? The answer to this is that once again, one can construct channels, at least, in principle. The construction proceeds along the same lines that were successful in constructing classical channels in numerical simulations for solid electrolytes,¹⁸ except that paths of higher than average dopant density (but still nearly constant in the channel) replace the electrolyte paths of higher than average atomic volume. Indeed, whenever there is competition between short- and long-range forces, one finds filamentary formation in classical models, including the cosmic web.²⁹ Because filaments are a topological property, there is no reason to suppose that this conclusion would be changed by quantum effects. Again, the branched conductive network is three dimensional. Finally, the long-range forces associated with intrafilamentary electron correlation can play a role similar to stress forces in glasses in determining the number of itinerant channel states $N-N_c \sim x-x_c$ over a wide range of $x > x_c$.

If the filamentary channels have restricted cross-sectional areas (limited by internal stresses), then, one can simply count wave function nodes between vertices to show that the number of itinerant states $N-N_c$ is proportional to the percolative volume obtained in fully relaxed and equilibrated glassy networks.²⁸ These free-carrier states must exist in the metallic phase, and their similarity to the cyclical mechanical modes of the model network glass²⁸ is certainly much more appealing than the analogy to critical fluctuations because the latter are relevant only very near one critical point, and in the present cases, there are certainly *two widely spaced* transitions at x_c and at $\sim 2x_c$.

In practice, the Fermi statistics (the additional complexities associated with antisymmetric wave functions) have prevented the identification of fermionic channels in numerical quantum simulations for randomly distributed impurities in three dimensions. However, at least qualitatively, it appears that near threshold approximately constant, higher-than-average density paths should be percolative (filamentary), as this process does not distinguish between real positive num-

bers (classical percolation) and complex numbers (quantum percolation). Note that the entropic objection to one-dimensional channels, which they cannot be metallic in the presence of weak disorder, is not valid for an *array* of weakly coupled or branched filaments.³⁰

VI. CONCLUSIONS

Our detailed discussion of the experimental data has shown that critical fluctuations fail to provide a consistent theory of the transport properties of these layered superconductors; instead, consistency requires a *nanoscopically inhomogeneous* model. The layered cuprate superconductors are also nanoscopically inhomogeneous. They share many percolative features with Li_xZrNCl , but at the same time, the latter shows a metal-insulator transition and an intermediate phase that resembles the one shown by semiconductor impurity bands, with σ proportional to $(x-x_c)^\alpha$, with $\alpha=0.5$. It is striking that the upper end of the quantum percolative range occurs near $x=2x_c$ in both the semiconductor impurity band case (where strain is not a factor) and Li_xZrNCl (where strain is the limiting factor). In the cuprate case, very large T_c are achieved by forcing the current carrying paths in CuO_2 planes to connect through soft dopants (usually interstitial oxygen) located between these rigid planes.^{16,33} This structural model has recently been confirmed in detail by STM studies.³¹ There is considerable further similarity between the phase diagrams of these three apparently different material families, as the broadening of the impurity band bound states to reach the continuum limit ($E=0$, or the band edge) at $x=2x_c$ in the semiconductor case corresponds to approxi-

mate equality of the superconductive and pseudogaps near optimal doping in the cuprates.

In the early days, Wilson proposed an alternative misfit structural model for the cuprates, based on intralayer currents entirely confined in metallic CuO_2 planar nanodomain walls flowing around insulating nanodomain islands.³² That misfit model appears to be realized in Li_xMNCl , which is especially gratifying, as it is complementary to the interlayer filamentary model³³ now deemed most appropriate to the cuprates. The differences between these two apparently quite similar layer topologies reflect the combined differences between rigid M^{+4} ions and ultraflexible Cu^{+2} , as well as donor Li^+ outside the sandwich, and acceptor O^- inside the sandwich.

Detailed and careful analysis of the data has shown that *homogeneous* continuum models based on critical fluctuations⁵ are simplistic and *cannot provide* satisfactory explanations for any of the observations. By contrast, quantum percolation⁶ in a soft, marginally stable (fragile) network accounts for all the observations in a realistic and unified theoretical framework. This framework shows that within the family of complex electronic networks, layered Li_xMNCl provides the missing link between the onset of quantum percolation at the metal-insulator transition, the $[x_c, 2x_c]$ intermediate phase in three-dimensional semiconductor impurity bands, and quantum percolation and the intermediate phase in the layered cuprates, which are responsible for high-temperature superconductivity,¹⁷ represented in Li_xMNCl by ΔT_c .

Note added. The present misfit model for Li_xMNCl suggests that it might be interesting to evaporate films with $M=\text{Zr}$, $a=0.361$ nm and $M=\text{Hf}$, $a=0.357$ nm; on MgCl_2 substrates,³⁴ $a=0.3596$ nm.

-
- ¹J. G. Bednorz and K. A. Mueller, Z. Phys. B: Condens. Matter **64**, 189 (1986).
²H. Kawaji, K. Hotehama, and S. Yamanaka, Chem. Mater. **9**, 2127 (1997).
³S. Yamanaka, K. Hotehama, and H. Kawaji, Nature (London) **392**, 580 (1998).
⁴Y. Taguchi, A. Kitora, and Y. Iwasa, Phys. Rev. Lett. **97**, 107001 (2006).
⁵P. A. Lee and T. V. Ramakrishnan, Rev. Mod. Phys. **57**, 287 (1985). However, for an earlier nanoscopic model, see J. C. Phillips, Solid State Commun. **47**, 191 (1983); see also M. Watanabe, Y. Ootuka, K. M. Itoh, and E. E. Haller, Phys. Rev. B **58**, 9851 (1998).
⁶J. C. Phillips, Solid State Commun. **109**, 301 (1999); M. Lee, A. Husmann, T. F. Rosenbaum, and G. Aeppli, Phys. Rev. Lett. **92**, 187201 (2004).
⁷Y. Meir, Phys. Rev. Lett. **83**, 3506 (1999); Y. Dubi, Y. Meir, and Y. Avishai, *ibid.* **94**, 156406 (2005).
⁸J. C. Phillips, Proc. Natl. Acad. Sci. U.S.A. **95**, 7264 (1998); P. Boolchand, G. Lucovsky, J. C. Phillips, and M. F. Thorpe, Philos. Mag. **85**, 3823 (2005).
⁹M. V. Koudriachova, N. M. Harrison, and S. W. de Leeuw, Phys. Rev. B **65**, 235423 (2002).
¹⁰F. Gligor and S. W. de Leeuw, Solid State Ionics **177**, 2741 (2006).
¹¹R. Heid and K. P. Bohnen, Phys. Rev. B **72**, 134527 (2005); H. Tou, Y. Maniwa, and S. Yamanaka, *ibid.* **67**, 100509(R) (2003).
¹²X. Chen, T. Koiwasaki, and S. Yamanaka, J. Solid State Chem. **159**, 80 (2001).
¹³Y. Taguchi, A. Kitora, M. Hisakabe, and Y. Iwasa, Physica B **383**, 67 (2006).
¹⁴T. Ekino, T. Takasaki, T. Muranaka, H. Fujii, J. Akimitsu, and S. Yamanaka, Physica B **328**, 23 (2003).
¹⁵H. J. Choi, M. L. Cohen, and S. G. Louie, Phys. Rev. B **73**, 104520 (2006).
¹⁶J. C. Phillips, Philos. Mag. B **81**, 35 (2001); **82**, 1163 (2002); Phys. Rev. B **71**, 184505 (2005); Philos. Mag. **83**, 3255 (2003); **83**, 3267 (2003).
¹⁷F. Wang, S. Mamedov, P. Boolchand, B. Goodman, and M. Chandrasekhar, Phys. Rev. B **71**, 174201 (2005); J. C. Phillips, *ibid.* **75**, 214503 (2007).
¹⁸St. Adams and J. Swenson, Phys. Rev. Lett. **84**, 4144 (2000).
¹⁹H. Darhmaoui and J. Jung, Phys. Rev. B **53**, 14621 (1996); J. C. Phillips and J. Jung, Philos. Mag. B **81**, 745 (2001).
²⁰K. M. Lang, V. Madhavan, J. E. Hoffman, E. W. Hudson, H. Eisaki, S. Uchida, and J. C. Davis, Nature (London) **415**, 412

- (2002).
- ²¹J. M. Vandenberg and B. T. Matthias, *Science* **198**, 194 (1977).
- ²²Y. Ando, G. S. Boebinger, A. Passner, L. F. Schneemeyer, T. Kimura, M. Okuya, S. Watauchi, J. Shimoyama, K. Kishio, K. Tamasaku, N. Ichikawa, and S. Uchida, *Phys. Rev. B* **60**, 12475 (1999); B. Brandow, *Phys. Rep.* **296**, 1 (1998); A. Junod, A. Erb, and C. Renner, *Physica C* **317**, 333 (1999).
- ²³Yu. N. Ovchinnikov and V. Z. Kresin, *Phys. Rev. B* **54**, 1251 (1996).
- ²⁴N. Kobayashi, S. Ikehata, S. Kobayashi, and W. Sasaki, *Solid State Commun.* **24**, 67 (1977).
- ²⁵D. Mihailovic, P. Kusar, J. Demsar, and V. V. Kabanov, *J. Supercond. Novel Magn.* **19**, 43 (2006).
- ²⁶A. Kitora, Y. Taguchi, and Y. Iwasa, *J. Phys. Soc. Jpn.* **76**, 023706 (2007).
- ²⁷R. Zallen and H. Scher, *Phys. Rev. B* **4**, 4471 (1971).
- ²⁸See Fig. 2 of H. He and M. F. Thorpe, *Phys. Rev. Lett.* **54**, 2107 (1985). The linear simplicity obtained in this glassy model is not found in lattice models of percolative phase transitions, which suggests that the simplicity of the intermediate phase is derived from its properly equilibrated glassy character, as explicitly demonstrated by Fig. 6 of M. V. Chubynsky, M. A. Briere, and N. Mousseau, *Phys. Rev. E* **74**, 016116 (2006).
- ²⁹C. Reichhardt, C. J. Olson Reichhardt, I. Martin, and A. R. Bishop, *Phys. Rev. Lett.* **90**, 026401 (2003); E. Kaneshita, I. Martin, and A. R. Bishop, *J. Phys. Soc. Jpn.* **73**, 3223 (2004); J. Barre, A. R. Bishop, T. Lookman, and A. Saxena, *Phys. Rev. Lett.* **94**, 208701 (2005); C. Reichhardt, C. J. O. Reichhardt, and A. R. Bishop, *Europhys. Lett.* **72**, 444 (2005); P. S. Salmon, *J. Phys.: Condens. Matter* **18**, 11443 (2006); J. C. Phillips, *Philos. Mag.* **B 81**, 757 (2001); M.-A. Briere, M. V. Chubynsky, and N. Mousseau, *Phys. Rev. E* (to be published); B. Schwarzschild, *Phys. Today* **60**(3), 20 (2007).
- ³⁰H. C. F. Martens, *Phys. Rev. Lett.* **96**, 076603 (2006).
- ³¹Y. Kohsaka, C. Taylor, K. Fujita, A. Schmidt, C. Lupien, T. Hanaguri, M. Azuma, M. Takano, H. Eisaki, H. Takagi, S. Uchida, and J. C. Davis, *Science* **315**, 1380 (2007).
- ³²J. A. Wilson, *Rep. Prog. Phys.* **60**, 941 (1997).
- ³³J. C. Phillips, *Phys. Rev. B* **41**, 8968 (1990).
- ³⁴H. Sano, H. Miyaoka, T. Kuze, H. Mori, G. Mizutani, N. Otsuka, and M. Terano, *Surf. Sci.* **502**, 70 (2002).